SUPPORTING INFORMATION

Chemical shift anisotropy of imino ^{15}N nuclei in Watson-Crick base pairs from magic angle spinning liquid crystal NMR and nuclear spin relaxation

Alexander Grishaev, Lishan Yao, Jinfa Ying, Arthur Pardi and Ad Bax

Laboratory of Chemical Physics, NIDDK, National Institutes of Health, Bethesda, Maryland 20892-0520 and Department of Chemistry and Biochemistry, University of Colorado, Boulder, CO 80309-0215

Data analysis

Uniform ^{15}N CSA tensor parameters for all G:N_1 and for all U:N_3 atoms in $tRNA^{Val}$ were fitted, assuming the CSA tensor to be symmetric with respect to the base plane, thus requiring three parameters to describe the traceless tensor (magnitudes of the out-of plane and one of the in-plane components, and the signed angle of the in-plane component with respect to the bisector of the heavy atom angle centered on the ^{15}N atom). The fit to the experimental data included 14 G nucleotides (1,2,3,5,15,24,39,40,42,46,49,50,52,63) and 6 Us (4,7,12,29,64,67). The tensors were fitted by Powell minimization of the χ^2 value calculated from the experimental and predicted data, weighted by the experimental data uncertainties. The experimental data included both the RCSA $\Delta\delta(^{15}N)$ values from the Pf1 alignment and the R_2/Γ ratios measured at 500 and 800 MHz. Data uncertainties are listed in Table S1. The alignment tensor for the Pf1 data was SVD-fitted to the previously reported structure of the $tRNA^{Val}$ refined against RDC and SAXS data (PDB code 1K4C). An axially symmetric anisotropic rotational diffusion tensor, corresponding to four adjustable parameters, was determined for the 1K4C model by minimizing the difference between observed and predicted 500 and 800 MHz R_1/R_2 and R_2/R_1 ratios of the 20 G:N_1 and U:N_3 sites. For this purpose, Powell minimization was used starting from the parameters predicted from the 1K4C model using HydroNMR software, with the χ value weighted by the propagated uncertainties of the R_2/R_1 and R_1/R_2 ratios, calculated from the respective uncertainties of the R_1 and R_2 rates. Since predicted relaxation rates depend on the parameters of the G:N_1 and U:N_3 CSA tensors, the rotational diffusion tensor fit procedure was run iteratively until convergence was reached, concurrently with the CSA tensor fitting procedure. In the first cycle, CSA parameters of the G:N_1 and U:N_3 were determined from the anisotropic shifts data alone. These values were then input in the procedure for the rotational diffusion tensor fit, producing its first estimate. The parameters of the rotational diffusion tensor were then input into the CSA tensor fit procedure, and these fits were performed against the observed $\Delta\delta(^{15}N)$ values (between aligned and isotropic states) and the R_2/Γ ratios measured at both 500 and 800 MHz. The resulting updated parameters of the CSA tensors were then input into the rotational diffusion tensor fit program which returned their updated estimate. Three iterations of this cycle were used to obtain complete convergence of the parameters for the rotational diffusion and CSA tensors. The final parameters of the CSA tensors are reported in Table 1 of the main text. The δ_{33} component is orthogonal to the base plane and the angle β is between the δ_{11} component and the bisector of the heavy atom angle (C_2-N_1-C_6 for G and C_2-N_3-C_4 for U). The positive sign of the angle corresponds to the left-handed rotation around the tensor product of the N_1-C_2 and N_1-C_6 vectors for G and N_3-C_2 and N_3-C_4 vectors for U (yielding the approximate δ_{22} orientations shown in the insets of Figure 2, main text).

The uncertainties in the average values of the CSA tensor components, reported in the main text Table 1, were estimated from 10,000 Monte Carlo runs, which added normally distributed random noise that matches data uncertainties of Table S1 to the fitted data, and 5° r.m.s. normally distributed random noise to the orientations of the individual base plane frames. These sets of noise-contaminated synthetic data were used as input for the fitting procedure described above for the experimental data. In these Monte-Carlo calculations, no attempts were made to iteratively refine the rotational diffusion tensor as

from a few trials it was clear that the impact of very small variations in the resulting diffusion tensor on the derived CSA values was negligible.

Site-specific relaxation rates were calculated from the CSA and rotational diffusion tensors and the structure using the following equations:

$$R_{1,i} = R_1^{CSA} + \sum_{r_{ij}<4A} R^{dip}{}_{1,ij}$$

$$R_{2,i} = R_2^{CSA} + \sum_{r_{ij}<4A} R^{dip}{}_{2,ij}$$

where the summation for nitrogen *i* extends over all other magnetically active nuclei, *j*, less than 4 Å from *i*.

$$\Gamma_i = \frac{R_2^{CSA,anti-TROSY} - R_2^{CSA,TROSY}}{2}$$

where $R_2^{CSA,anti\text{-}TROSY}$ and $R_2^{CSA,\text{-}TROSY}$ are the transverse relaxation rates calculated for the upfield and downfield doublet components, assuming a pseudo-CSA tensor that equals the sum or difference of the dipolar and regular CSA tensor. Calculation of the CSA-based relaxation rates follows below.

$$R_1^{CSA} = \omega_N^2 G(\omega_N, CSA, Dxx, Dyy, Dzz, \alpha, \beta, \gamma)$$

$$R_2^{CSA} = \omega_N^2 \left[4G(0, CSA, Dxx, Dyy, Dzz, \alpha, \beta, \gamma) + 3G(\omega_N, CSA, Dxx, Dyy, Dzz, \alpha, \beta, \gamma)\right]$$

$$R_2^{CSA,TROSY} = \omega_N^2 \left[4G(0, CSA^{TROSY}, Dxx, Dyy, Dzz, \alpha, \beta, \gamma) + 3G(\omega_N, CSA^{TROSY}, Dxx, Dyy, Dzz, \alpha, \beta, \gamma)\right]$$

$$R_2^{CSA,antiTROSY} = \omega_N^2 \left[4G(0, CSA^{antiTROSY}, Dxx, Dyy, Dzz, \alpha, \beta, \gamma) + 3G(\omega_N, CSA^{antiTROSY}, Dxx, Dyy, Dzz, \alpha, \beta, \gamma)\right]$$

Above, Dxx, Dyy, Dzz are the eigenvalues of the rotational diffusion tensor and α, β, γ are the Euler angles for the rotation between the CSA frame and the frame of the rotational diffusion tensor. The TROSY CSA tensor is defined as a difference of the N-H dipolar and ^{15}N CSA tensors and anti-TROSY CSA tensor as their sum.

$$G(\omega, CSA, Dxx, Dyy, Dzz, \alpha, \beta, \gamma) = \sum_{i=1}^{5} \frac{c_i \tau_i}{1 + \omega^2 \tau_i^2}$$

$$c_1 = \frac{1}{40}\left(3\sin^2(\beta)\sin(2\gamma) - \eta_\lambda(\cos(2\alpha)\sin(2\gamma)(\cos^2(\beta) - 1) + 2\sin(2\alpha)\cos(\beta)\cos(2\gamma))\right)^2 \Delta_\lambda{}^2$$

$$c_2 = \frac{1}{40}\left(3\sin(2\beta)\cos(\gamma) + \eta_\lambda(\cos(2\alpha)\sin(2\beta)\cos(\gamma) - 2\sin(2\alpha)\sin(\beta)\sin(\gamma))\right)^2 \Delta_\lambda{}^2$$

$$c_3 = (1.5(1+A)(3\cos^2(\beta)-1-\eta_\lambda \sin^2(\beta)\cos(2\alpha)-0.5\eta_D(3\sin^2(\beta)\cos(2\gamma)-\eta_\lambda(\cos(2\alpha)\cos(2\gamma)(\cos^2(\beta)+1)-2\sin(2\alpha)\sin(2\gamma)\cos(\beta))))^2 \frac{\Delta_\lambda^2}{60A(1+A)}$$

$$c_4 = \frac{1}{40}\left(3\sin(2\beta)\sin(\gamma)+\eta_\lambda(\cos(2\alpha)\sin(2\beta)\sin(\gamma)+2\sin(2\alpha)\sin(\beta)\cos(\gamma))\right)^2 {\Delta_\lambda}^2$$

$$c_5 = (-0.5\eta_D(3\cos^2(\beta)-1-\eta_\lambda \sin^2(\beta)\cos(2\alpha))+0.5(1+A)(3\sin^2(\beta)\cos(2\gamma)-\eta_\lambda(\cos(2\alpha)\cos(2\gamma)(\cos^2(\beta)+1)-2\sin(2\alpha)\sin(2\gamma)\cos(\beta))))^2 \frac{\Delta_\lambda^2}{20A(1+A)}$$

$$\tau_1 = \frac{1}{6D_s\left(1+\frac{D^*}{2D_s}\right)}$$

$$\tau_2 = \frac{1}{6D_s\left(1-\frac{D^*(1-\eta_D}{4D_s}\right)}$$

$$\tau_3 = \frac{1}{6D_s\left(1-\frac{D^*A}{2D_s}\right)}$$

$$\tau_4 = \frac{1}{6D_s\left(1-\frac{D^*(1+\eta_D}{4D_s}\right)}$$

$$\tau_5 = \frac{1}{6D_s\left(1+\frac{D^*A}{2D_s}\right)}$$

where

$$\Delta_\lambda = \delta_{33} * 10^{-6}$$

$$\eta_\lambda = \frac{\delta_{22} - \delta_{11}}{\delta_{33}}$$

$$D_s = \frac{D_{xx} + D_{yy} + D_{zz}}{3}$$

$$D^* = D_{zz} - D_s$$

$$\eta_D = \frac{D_{yy} - D_{xx}}{D*}$$

$$A = \sqrt{1 + \frac{\eta_D{}^2}{3}}$$

Calculation of the dipolar-based relaxation rates follows below.

$$R^{dip}{}_{1,ij} = (3J_{sym}(\omega_N, \alpha, \tau_1, \tau_2, \tau_3) + J_{sym}(\omega_j - \omega_N, \alpha, \tau_1, \tau_2, \tau_3) + 6J_{sym}(\omega_j + \omega_N, \alpha, \tau_1, \tau_2, \tau_3))\frac{\xi_{ij}^2}{4}$$

$$R^{dip}{}_{1,ij} = (4J_{sym}(0, \alpha, \tau_1, \tau_2, \tau_3) + 3J_{sym}(\omega_N, \alpha, \tau_1, \tau_2, \tau_3) +$$

$$+ J_{sym}(\omega_j - \omega_N, \alpha, \tau_1, \tau_2, \tau_3) + 6J_{sym}(\omega_j, \alpha, \tau_1, \tau_2, \tau_3) + 6J_{sym}(\omega_j + \omega_N, \alpha, \tau_1, \tau_2, \tau_3))\frac{\xi_{ij}^2}{8}$$

Above, α is the angle between the i-j dipolar vector and the Dzz axis of the axially symmetric diffusion tensor and

$$\tau_1 = \frac{1}{6D_{xx}}$$

$$\tau_2 = \frac{1}{5D_{xx} + D_{zz}}$$

$$\tau_3 = \frac{1}{2D_{xx} + 4D_{zz}}$$

$$\xi_{ij} = \frac{\mu_o h \gamma_N \gamma_j}{8\pi^2 r_{ij}^3}$$

$$J_{sym}(\omega,\alpha,\tau_1,\tau_2,\tau_3) = 0.25(3\cos^2(\alpha)-1)^2\,\frac{0.4\tau_1}{1+\omega^2\tau_1^2} + 3\cos^2(\beta)\sin^2(\beta)\frac{0.4\tau_2}{1+\omega^2\tau_2^2} + 0.75\sin^4(\beta)\frac{0.4\tau_3}{1+\omega^2\tau_3^2}$$

Supporting Information Table S1. Experimental data used for derivation of the CSA tensors of U:N3 and G:N1.

	Δδ, ppb[b]	R_1^{800}, Hz	R_1^{500}, Hz	R_2^{800}, Hz	R_2^{500}, Hz	Γ^{800}, Hz	Γ^{500},Hz
U4	-29.721	0.386±0.017	0.730±0.028	25.18±0.86	21.21±0.66	17.50±0.23	11.20±0.23
U7	-0.320	0.350±0.017	0.751±0.028	23.44±0.86	18.78±0.66	16.30±0.23	10.00±0.23
U12	-37.909	0.345±0.017	0.727±0.028	25.62±0.86	21.46±0.66	n.a.	n.a.
U29	-98.610	0.421±0.017	0.815±0.028	21.91±0.86	16.21±0.66	15.70±0.23	n.a.
U64	45.803	0.322±0.017	0.631±0.028	29.24±0.86	23.41±0.66	22.60±0.23	14.10±0.23
U67	-49.670	0.395±0.017	0.777±0.028	20.78±0.86	16.34±0.66	12.90±0.23	8.10±0.23
G1	1.321	0.507±0.031	0.841±0.047	24.02±1.17	18.61±0.87	18.30±0.56	11.80±0.54
G2	11.268	0.419±0.031	0.803±0.047	27.00±1.17	20.38±0.87	21.90±0.56	14.40±0.54
G3	-3.935	0.396±0.031	0.747±0.047	27.34±1.17	19.94±0.87	n.a.	n.a.
G5	-89.367	0.453±0.031	0.867±0.047	23.90±1.17	18.50±0.87	18.20±0.56	11.30±0.54
G15	-83.948	0.507±0.031	0.978±0.047	23.38±1.17	19.06±0.87	17.00±0.56	n.a.
G24	-61.895	0.361±0.031	0.825±0.047	24.87±1.17	21.42±0.87	20.70±0.56	13.00±0.54
G39	-65.866	0.374±0.031	0.829±0.047	25.87±1.17	19.06±0.87	n.a.	12.30±0.54
G40	-89.155	0.476±0.031	0.916±0.047	23.77±1.17	17.19±0.87	18.90±0.56	11.10±0.54
G42	-32.307	0.433±0.031	0.849±0.047	24.71±1.17	19.22±0.87	n.a.	13.70±0.54
G46	-93.701	0.441±0.031	0.798±0.047	22.59±1.17	18.94±0.87	19.10±0.56	12.10±0.54
G49	58.397	0.303±0.031	0.697±0.047	33.16±1.17	24.11±0.87	25.90±0.56	n.a.
G50	33.123	0.355±0.031	0.682±0.047	28.61±1.17	23.84±0.87	25.40±0.56	15.90±0.54
G52	-60.255	0.432±0.031	0.882±0.047	22.26±1.17	17.66±0.87	16.10±0.56	10.30±0.54
G63	42.548	0.372±0.031	0.859±0.047	27.22±1.17	21.06±0.87	21.70±0.56	13.70±0.54

Supporting Information Table S2. Temperature coefficients of imino (G:N_1-H; U:N_3-H) ^{1}H and ^{15}N resonances in $tRNA^{Val}$.

	^{1}H ppb/K	^{15}N ppb/K
G1	0.85	9.65
G2	-1.74	1.42
G3	-1.76	3.60
U4	-3.95	-1.57
G5	-2.46	6.02
U7	-3.09	-0.79
s^4U8	-4.20	-6.21
G10	-2.08	9.17
U12	-4.38	0.22
G15	-3.36	4.81
G22	-2.82	2.71
G24	-3.18	5.96
U29	-3.24	-4.45
G39	-0.19	5.33
G40	-2.41	4.55
G42	-2.45	4.96
m^7G46	-1.34	6.53
G49	-1.88	2.15
G50	-4.45	2.24
G52	-2.80	5.08
G53	-1.66	6.15
T54	-3.32	-3.29
Ψ55 (N3)	-0.84	-0.91
G63	-1.56	6.43
U64	-2.05	-0.37
U67	-5.26	-2.89

[a] The temperature coefficients were measured from two HSQC spectra recorded using identical acquisition parameters at 298 K and 303 K on a Bruker Avance 500 spectrometer equipped with a z-axis gradient triple resonance cryogenic probe, with the carrier frequency calibrated relative to 10 μM internal TSP. The proton temperature coefficient is then calculated as:

$$^{1}H_{coeff} = (\delta_{303K} - \delta_{298K})/(303K - 298K).$$

The ^{15}N chemical shift temperature coefficients were calculated similarly, using the IUPAC-recommended method of indirectly referencing the ^{15}N spectrum to the internal ^{1}H standard.

Supporting Information Table S3. Comparison of the derived CSA parameters with the results of previous studies.

		β,°	δ_{11}, ppm	δ_{22}, ppm	δ_{33}, ppm
$G:N_1$	This study	13.1±1.4	77.9±1.7	-12.4±2.2	-65.5±2.5
	Ref 1 (ab initio, R_{NN}=2.87 Å)	18.9	66.8	-1.6	-65.1
	Ref 1 (ab initio, R_{NN}=3.02 Å)	16.6	66.6	-8.1	-58.4
	Ref 2 (ab initio, R_{NN}=2.85 Å)	19.1	80.2	-3.9	-76.3
	Ref 2 (ab initio, R_{NN}=3.05 Å)	16.1	79.9	-13.6	-66.3
	Ref 3 (SS NMR)	3±6	66.7	13.7	-80.3
	Ref 4 (SS NMR)		82.8	-4.1	-78.7
$U:N_3$	This study	11.4±2.4	68.5±1.6	2.3±2.9	-70.8±3.2
	Ref 2 (ab initio, R_{NN}=2.75 Å)	20.4	64.4	15.8	-80.3
	Ref 2 (ab initio, R_{NN}=2.85 Å)	17.1	64.5	9.6	-74.0
	Ref 5 (SS NMR)	9	64.0	-6.0	-58.0
	Ref 6 (SS NMR)	15	66.4	-2.8	-63.6

References:

1. J. Czernek, R. Fiala, V. Sklenar, J. Magn. Reson., **2000**, *145*, 142-146.
2. J. Czerek, *J. Phys. Chem. A.,* **2001**, *105*, 1357-1365.
3. G. Lorigan, R. McNara, R. Jones, S. Opella, *J. Magn. Reson.,* **1999**, *140*, 315-319.
4. D. Steuber, D. Grant, *J. Am. Chem. Soc*., **2002**, *124*, 10539-10551.
5. K. Anderson-Altmann, C. Phung, S. Mavromoustakos, Z. Zheng, J. Facelli, C. Poulter, D. Grant, *J. Phys. Chem.,* **1995**, *99*, 10454-10458.
6. J. Leppert, B. Heise, R. Ramachandran, *J. Magn. Reson.*, **2000**, *145*, 307-314.

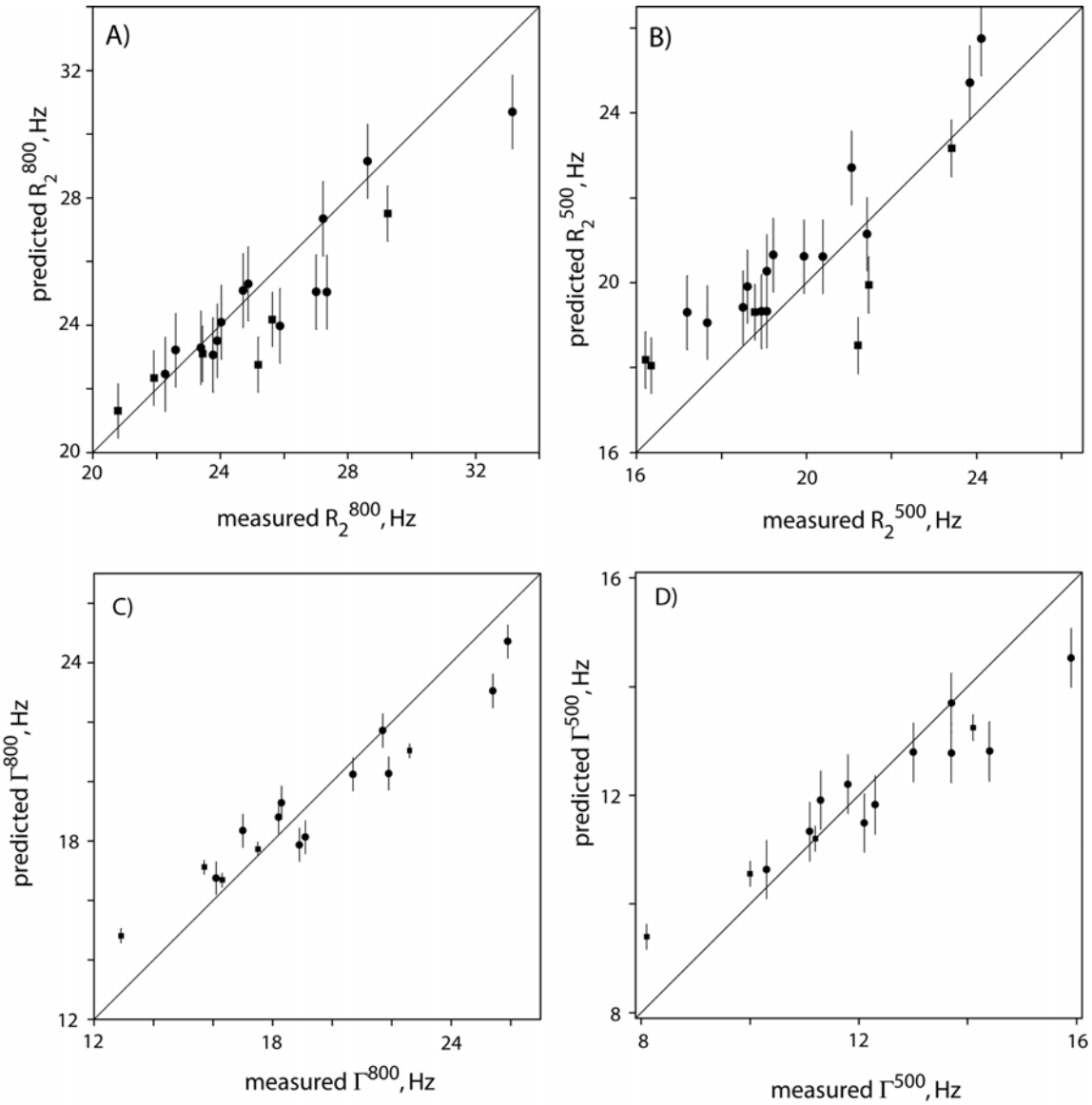

Supporting Information Figure S1. Correlation of experimental relaxation rates and those predicted based on the structural model and fitted CSA tensors. R_2^{800} (panel A), R_2^{500} (panel B), Γ^{800} (panel C), and Γ^{500} (panel D) data are shown. Squares denote U:N_3 data and circles correspond to G:N_1 data.

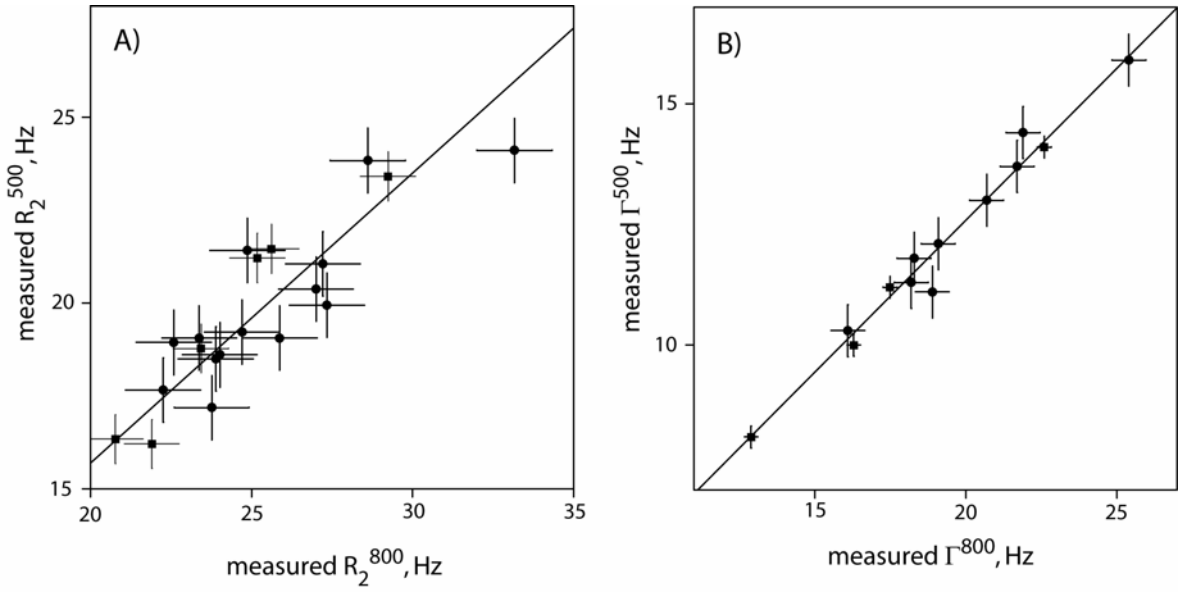

Supporting Information Figure S2. Correlation between R_2 (panel A) and Γ (panel B) rates at 500 and 800 MHz. The individual data uncertainties are indicated by the error bars. $U:N_3$ data are shown as squares and $G:N_1$ as circles. The correlation coefficients in linear regression fits shown as lines are $R^2 = 0.77$ for panel A and $R^2 = 0.975$ for panel B.

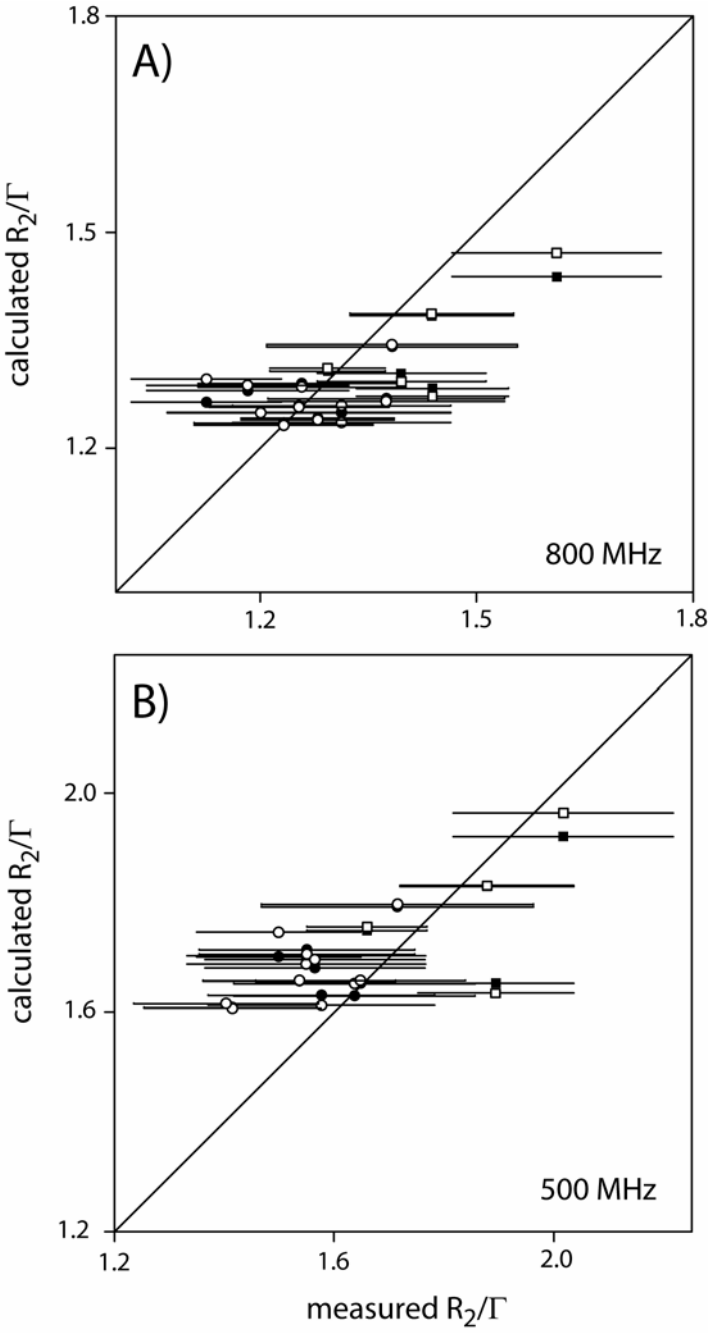

Supporting Information Figure S3. Correlations between the experimental and calculated values for the R2/Γ ratios. Data at 800 MHz are shown in panel A and at 500 in panel B. Filled symbols correspond to the results of the fit and open symbols correspond to the results of a jack-knifed cross-validation procedure. Circles denote G:N_1 and squares denote U:N_3. Horizontal error bars indicate the uncertainties of the experimental R2/Γ ratios.